Hybrid adaptive optics system for a solid-state zigzag master oscillator power amplifier laser system

Boheng Lai (赖柏衡)[1,2,3], Lizhi Dong (董理治)[1,2], Shanqiu Chen (陈善球)[1,2], Guomao Tang (汤国茂)[1,2], Wenjin Liu (刘文劲)[1,2], Shuai Wang (王 帅)[1,2], Xing He (何 星)[1,2], Kangjian Yang (杨康建)[1,2,3], Ping Yang (杨 平)[1,2,*], Bing Xu (许 冰)[1,2,], Chao Wang (王 超)[4], Xianda Liu (刘先达)[4], Qingsheng Pang (庞庆生)[4], and Yang Liu (刘 洋)[4]**

[1]*Key Laboratory on Adaptive Optics, Chinese Academy of Sciences, Chengdu 610209, China*
[2]*Institute of Optics and Electronics, Chinese Academy of Sciences, Chengdu 610209, China*
[3]*University of Chinese Academy of Sciences, Beijing 100049, China*
[4]*Institute of North Optics and Electronic, Beijing 100015, China*
**Corresponding author: pingyang2516@163.com; **corresponding author: bing_xu_ioe@163.com*
Received February 28, 2016; accepted July 1, 2016; posted online July 25, 2016

We present a hybrid adaptive optics system for a kW-class solid-state slab master oscillator power amplifier laser that consists of both a low-order aberration corrector and a 59-actuator deformable mirror. In this system large defocus and astigmatism of the beam are first corrected by the low-order aberration corrector and then the remaining components are compensated by the deformable mirror. With this sequential procedure it is practical to correct the phase distortions of the beam (peak to valley up to 100 μm) and the beam quality β is successfully improved to 1.9 at full power.

OCIS codes: 010.1080, 140.5680, 090.1000.
doi: 10.3788/COL201614.091402.

Recent years have witnessed great progress in solid-state lasers (SSLs)[1,2]. Higher output power and higher beam qualities have always been the major demand. Since zigzag slab lasers[3] have been invented they have become one of the most promising architecture for power scaling of SSLs thanks to their advantageous pumping, cooling, and power extraction geometries[4,5]. Although heat gradients could be averaged by propagating the beam in the zigzag scheme there are still significant phase aberrations in the non-zigzag direction, leading to different divergence angles in both directions[6], or large defocus and astigmatism described with phase aberrations. Furthermore, non-uniform pumping and heat removal will also bring in phase distortions that all contribute to deteriorated beam qualities. Since these aberrations vary with pumping power and continuously grow before a balanced state of temperature distribution is reached they cannot be simply eliminated with static devices such as lens systems or phase plates. As adaptive optics (AO) systems can compensate fast changing phase aberrations in real time[7,8], they have been successfully applied in slab laser systems[9].

Most reported AO systems for slab lasers solely use deformable mirrors (DMs) to correct the phase aberrations. However, the phase distortions of the output beam of slab lasers could be very large (peak to valley up to 100 μm), which is beyond the stroke of a conventional DM. A possible solution is to combine multiple conventional DMs or one-dimensional DMs[10,11]. However, employing more DMs can be very expensive and make the control system complicated. Previously we have reported an AO system for a slab laser system with a 39-actuator DM[12]. In this system two cylindrical lenses are used to expand the beam in the non-zigzag direction. As the divergence angles in the zigzag and non-zigzag direction are rather different, which will lead to a large defocus and astigmatism, the two cylindrical lenses also work as an astigmatism corrector and a large uncorrectable defocus still exists. Thus, in that system defocus is ignored. In addition, as the focal lengths of the cylindrical lenses are fixed, when the pump power changes the distance between the lenses must be adjusted and the size of the beam on the DM will also change.

In this Letter we present a hybrid AO system for a kW-class solid-state slab master oscillator power amplifier (MOPA) laser system. In this hybrid AO system, the phase aberration of the slab amplifier is first corrected by a low-order corrector that consists of cylindrical and spherical lenses, and the remaining components are then sent to the DM. With this hybrid system there is no need to develop a large stroke DM for the slab laser amplifier.

Figure 1 depicts the zigzag convention cooled end-pumped slab (CCEPS) laser amplifier[13] and the hybrid AO system. A single-mode continuous-wave (CW) fiber laser is used as the master oscillator of the MOPA system whose output beam is collimated and transformed into a rectangular aperture. Then the beam passes four Nd:YAG slab amplifiers in the zigzag configuration and achieves kW-class output. More details about the MOPA system can be found in Ref. [13]. First, the beam of the slab amplifier is corrected by the low-order corrector, which consists of cylindrical and spherical lenses fixed on a motorized rail. By adjusting the distances between these lenses this device can correct both defocus and

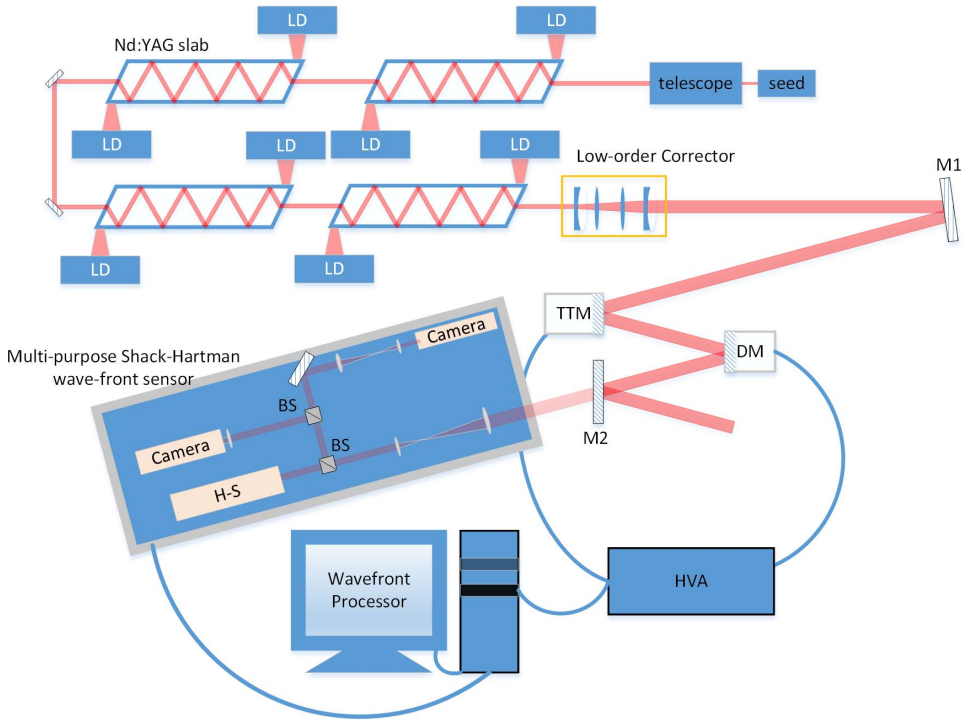

Fig. 1. Schematic of the hybrid AO system for the MOPA laser system.

astigmatism and the size of the beam could also be adaptively changed to fit the aperture of the DM, which is impossible with our previous system[9]. Then the beam is further corrected by both a tip/tilt mirror (TTM) and a continuous surface DM with discrete actuators, as is shown in Fig. 2(a). Finally, the output beam is sampled by a high-reflectivity (HR) mirror (M2) and measured by a multipurpose Shack–Hartman wavefront sensor (HS) that can also get the near-field and far-field intensity distributions of the beam, as is shown in Fig. 2(b).

As is constrained by the size of the beam, the largest number of achievable actuators is 59 in our lab. The distance between neighboring actuators of the DM is 8 mm, and the stroke of each actuator is 5 μm. The effective area of DM is 52 mm × 52 mm. Figure 3 shows the match of the 59 actuator to the subapertures of the lens arrays. The real-time wavefront processor receives images from the multipurpose HS and calculates the voltages for both the TM and the DM, and sends signals to the high-voltage amplifier (HVA). Both the TTM and the DM are directly driven by the HVA. The wavefront processor is based on a real-time Linux and x86 CPU and operates at the sample

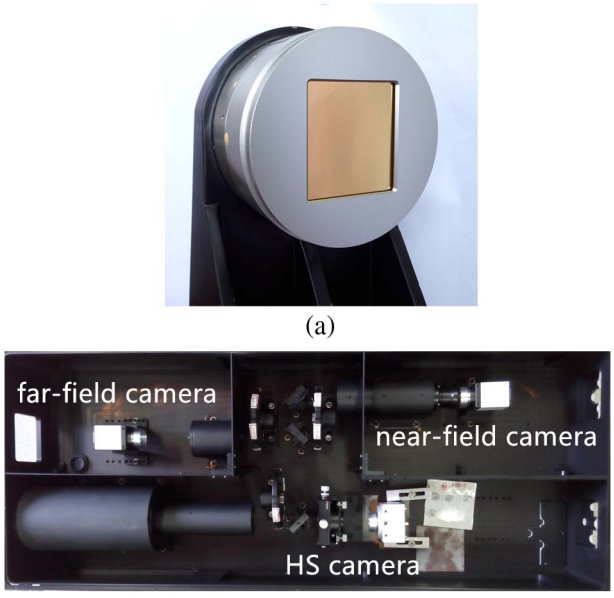

Fig. 2. (a) 59-actuator DM and (b) the multipurpose HS.

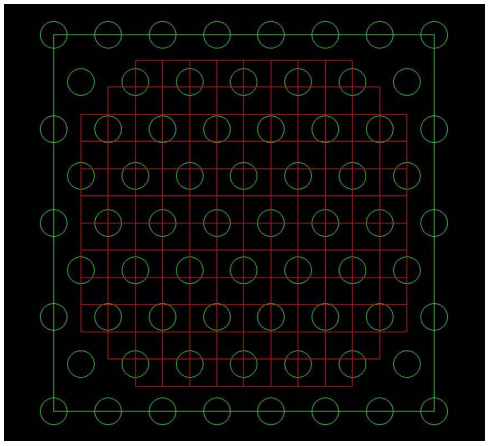

Fig. 3. HS aperture and the actuator positions in the AO system.

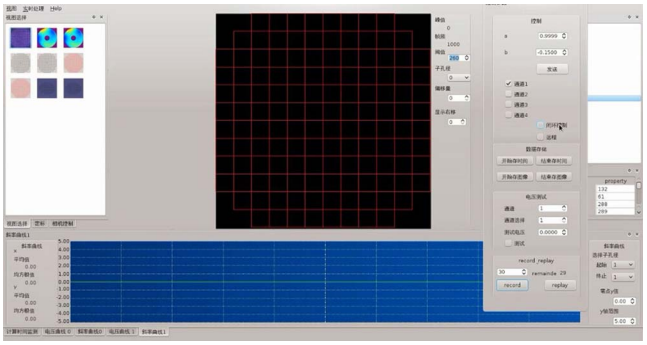

Fig. 4. Software interface of the wavefront processor.

rate of 1000 Hz[14]. The software interface of the processor is shown in Fig. 4. To correct a large defocus and astigmatism of the output laser to a low level, which is within the stroke of the DM, the spacing between the cylindrical and spherical lenses of the low-order corrector are first calculated according to the initial beam characteristics, then the lenses move to the calculated position.

After that, the laser system operates at the prescribed power and the distances between the lenses are further adjusted using the wavefront sensor as feedback. The low-order corrector can be reconfigured at different output powers of the laser system. Figure 5(a) shows the typical spots of the wavefront senor of the laser beam after the low-order corrector. Figure 5(b) illustrates the phase aberrations that are reconstructed with the zonal method using the Southwell model[15]. Then remaining components are corrected by the DM in real time. The strategy for the DM control system is a direct-gradient reconstruction algorithm[16].

The relationship between the HS and DM can be described as

$$G = F \cdot V, \tag{1}$$

where F is the reconstruction matrix of the direct-gradient algorithm that is determined by the structure of the HS and DM; V is the vector of voltage applied in the DM. G is the vector of the wavefront slopes of the x and y directions in all subapertures; G is measured by HS, and then V could be calculated from Eq. (2), where F^+ is the pseudoinverse of F:

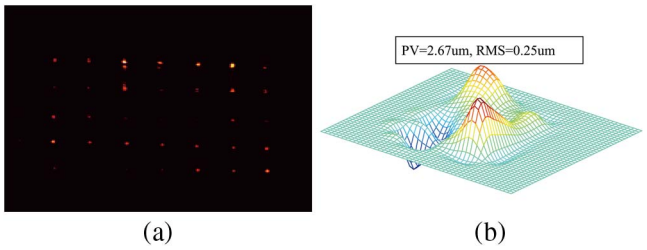

Fig. 5. (a) Typical spots of the wavefront senor of the laser beam and (b) the wavefront of laser beam.

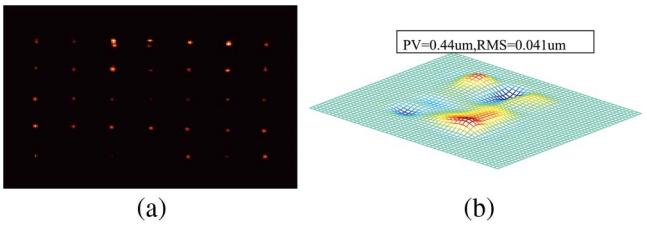

Fig. 6. (a) Typical spots of the wavefront senor of the laser beam when AO is on and (b) the wavefront of the laser beam.

$$V = F^+ \cdot G. \tag{2}$$

The surface of the DM could also be calculated according to V and influence the functions of the actuators.

We have done several experiments with the above hybrid AO system. Figure 6(a) shows the typical spots detected by the multipurpose wavefront sensor. Figure 6(b) shows that aberrations of the beam could be well corrected after sequential working of the low-order wavefront corrector and the DM.

Figure 7 shows the typical near-field spots of the laser beam at full power. We use β based on the power in bucket (PIB) to evaluate the beam quality, which is defined[17] as

$$\beta = \sqrt{\frac{A_{\text{real}}}{A_{DL}}}. \tag{3}$$

As the beam is almost square, we use a square PIB bucket instead of a circle, which is widely used for circular beams. A_{real} is the area of the actual beam containing 81.5% of the total power in the far field, while A_{DL} is the area containing 81.5% of the total power in the diffraction-limited case. Figure 8 illustrates the far-field intensity distribution of the beam after being corrected by the entire hybrid system. As is shown, the beam quality (β) has been successfully improved to 1.9. It should be noted that the peak intensity of the far-field spot is enhanced about 7 times after the DM is on. Figure 9 illustrates the PIB of the far field of the laser beam before and after the DM is on. It is clear that the power concentration of the beam is significantly improved after correction.

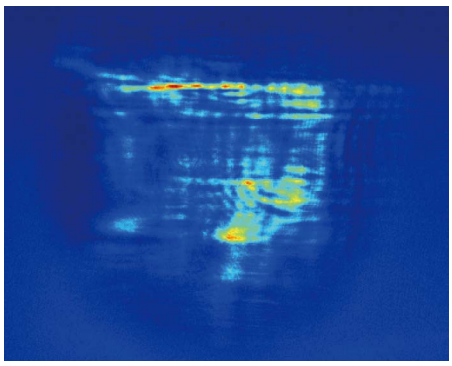

Fig. 7. Near-field of the laser beam at full power.

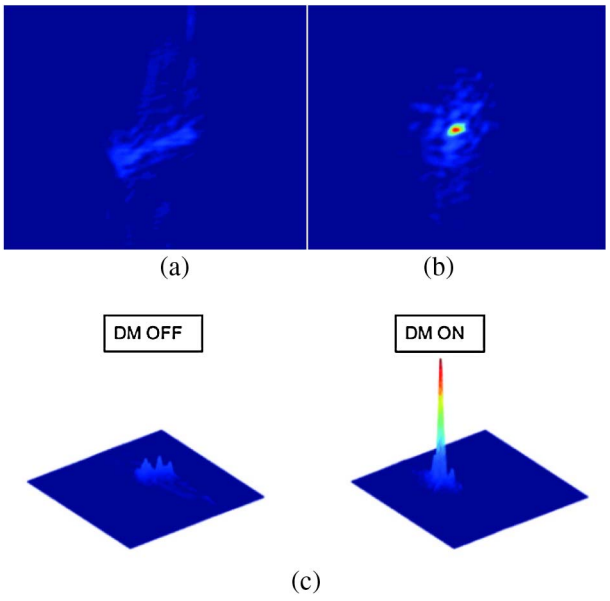

Fig. 8. (a) Far-field intensity distribution of the beam after the low-order compensator, $\beta = 7.3$. (b) The far-field intensity distribution of the beam after being corrected by the DM; $\beta = 1.9$. (c) The 3D figure of the far field of (a) and (b).

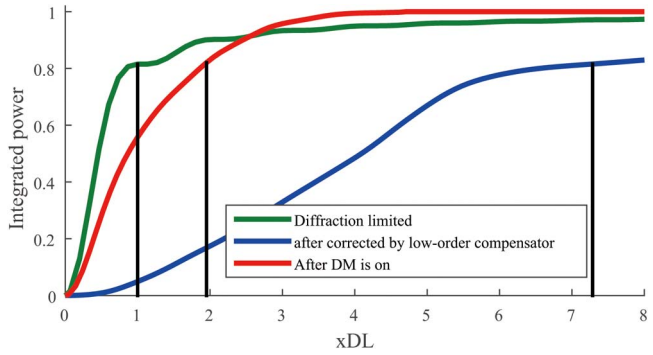

Fig. 9. PIB of the beam before and after the DM is on.

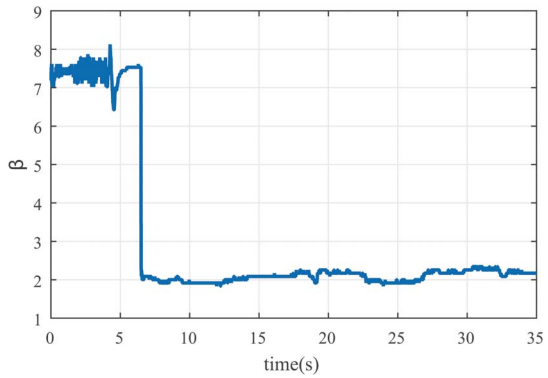

Fig. 10. β overall process of the laser's operation after the hybrid AO system.

The curve of the β overall process of the laser's operation is shown in Fig. 10. The average value after being corrected by the low-order corrector is 7.4. When the DM is on the average value improved to 2.1. During the whole process, the AO system worked stably.

In conclusion, the aberrations of a kW-class solid-state zigzag MOPA laser is successfully compensated by the hybrid AO system we presented. In this system large defocus and astigmatism of the beam are first corrected by the low-order corrector comprised of cylindrical and spherical lenses. Then the remaining components are compensated by the 59-actuator DM. The beam quality (β) is successfully improved to 1.9 under full power. Faced with a large distortion in the high power laser, the hybrid AO system offers an alternative choice.

This work was supported by the National Key Scientific Equipment Development Project of China under Grant No. ZDYZ2013-2.

References

1. R. M. Yamamoto, J. M. Parker, K. L. Allen, R. W. Allmon, K. F. Alviso, C. P. J. Barty, B. S. Bhachu, C. D. Boley, A. K. Burnham, R. L. Combs, K. P. Cutter, S. N. Fochs, S. A. Gonzales, R. L. Hurd, K. N. LaFortune, W. J. Manning, M. A. McClelland, R. D. Merrill, L. Molina, C. W. Parks, P. H. Pax, A. S. Posey, M. D. Rotter, B. M. Roy, A. M. Rubenchik, T. F. Soules, and D. E. Webb, Proc. SPIE **6552**, 655205 (2007).
2. R. Tao, P. Ma, X. Wang, P. Zhou, and Z. Liu, Photon. Res. **3**, 86 (2015).
3. H. Injeyan and G. Goodno, *High Power Laser Hand Book* (McGraw-Hill, 2011), p. 188.
4. A. Mandl and D. E. Klimek, IEEE J. Quantum Electron. **31**, 916 (1995).
5. G. D. Goodno, H. Komine, S. J. McNaught, S. B. Weiss, S. Redmond, W. Long, R. Simpson, E. C. Cheung, D. Howland, P. Epp, M. Weber, M. McClellan, J. Sollee, and H. Injeyan, Opt. Lett. **31**, 1247 (2006).
6. W. Koechner, *Solid-State Laser Engineering* (Springer, 1999).
7. Y. Yu and Y. Zhang, Chin. Opt. Lett. **12**, 121202 (2014).
8. C. Rao, L. Zhu, X. Rao, L. Zhang, H. Bao, L. Kong, Y. Guo, X. Ma, M. Li, C. Wang, X. Zhang, X. Fan, D. Chen, Z. Feng, X. Wang, N. Gu, and Z. Wang, Chin. Opt. Lett. **13**, 120101 (2015).
9. S. Redmond, S. McNaught, J. Zamel, L. Iwaki, S. Bammert, R. Simpson, S. B. Weiss, J. Szot, B. Flegal, T. Lee, H. Komine, and H. Injeyan, in *Conference on Lasers and Electro-Optics (CLEO)* (IEEE, 2007), Paper CTuHH5.
10. X. Lei, S. Wang, H. Yan, W. Liu, L. Dong, P. Yang, and B. Xu, Opt. Express **20**, 22143 (2012).
11. X. Rujian, Z. Kai, W. Jing, D. Yinglei, L. Zhongxiang, H. Zhongwu, and X. Honglai, Proc. SPIE **9255**, 92552Y (2015).
12. P. Yang, Y. Ning, X. Lei, B. Xu, X. Li, L. Dong, H. Yan, W. Liu, W. Jiang, L. Liu, C. Wang, X. Liang, and X. Tang, Opt. Express **18**, 7121 (2010).
13. H. Zhao, S. Zhou, X. Tang, L. Liu, C. Wang, C. Zhu, and L. Zhang, in *LASER 2012 Conference* (2012), Paper TN2 O43.
14. C. Shanqiu, L. Chao, X. Bing, and Y. Yutang, Chin. J. Lasers **42**, 1212001 (2015).
15. R. Tyson, *Principle of Adaptive Optics* (Taylor & Francis, 2011), p. 222.
16. W. Jiang and P. Yan, Acta Opt. Sin. **6**, 558 (1990).
17. G. Feng and S. Zhou, Chin. J. Lasers **36**, 1643 (2009).